SOLID-STATE SUPERCAPACITOR BASED ON POLYMER FILM SEPARATOR AND THERMAL COATED SILVER ELECTRODE

A DISSERTATION
SUBMITTED IN PARTIAL FULFILLMENT OF THE REQUIREMENTS
FOR THE AWARD OF DEGREE
OF

MASTER OF TECHNOLOGY IN
NANOSCIENCE AND TECHNOLOGY

Submitted by
SAURABH DARIPA
(Roll No. 2K18/NST/07)

Under the supervision of
DR. AMRISH K PANWAR
(ASSISTANT PROFESSOR)

DEPARTMENT OF APPLIED PHYSICS
Delhi Technological University (Formerly Delhi College of Engineering)
Bawana Road, Delhi-110042

JUNE,2020

DELHI TECHNOLOGICAL UNIVERSITY
(Formerly Delhi College of Engineering)
Bawana Road, Delhi-110042

CANDIDATE'S DECLARATION

I, SAURABH DARIPA, Roll No. 2K18/NST/07 of M.Tech. Nanoscience and Technology, hereby declare that the project Dissertation titled **"Solid-state supercapacitor based on polymer film separator and thermal coated Silver electrode"** which is submitted by me to the Department of Applied Physics, Delhi Technological University, Delhi in partial fulfillment of the requirement for the award of the degree of Master of technology, is original and not copied from any source without proper citation. This work has not previously formed the basis for the award of any Degree, Diploma Associate ship, Fellowship or other similar title or recognition.
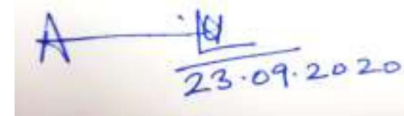
Place: Delhi, India

Date: 31-08-2020

Saurabh Daripa

DELHI TECHNOLOGICAL UNIVERSITY
(Formerly Delhi College of Engineering)
Bawana Road, Delhi-110042

CERTIFICATE

I hereby certify that the Project Dissertation titled **"Solid-state supercapacitor based on polymer film separator and thermal coated Silver electrode"** by Saurabh Daripa, Roll No. 2K18/NST/07, Department of Applied Physics, Delhi Technological University, Delhi in partial fulfillment of the requirement for the award of the degree of Master of Technology, is a record of the project work carried out by the student under my supervision. To the best of my knowledge, this work has not been submitted in part or full for any Degree or Diploma to this University or elsewhere.

23.09.2020

Place: Delhi, **Dr. Amrish K. Panwar**
Date: 23-09-2020 **Supervisor**

ACKNOWLEDGEMENT

With great pleasure and respect, I express my heartfelt gratitude to my supervisor **Dr. AMRISH K PANWAR, Assistant Professor, Applied Physics, Delhi Technological University** for his constant support, motivation and patience during my entire MTech dissertation. I'm very thankful to him for providing me with such excellent in-house lab facilities due to which I can complete my project.

I would also like to express my deepest regard to my parents for always supporting and standing by me in every decision of my life. Without their sacrifices and love I wouldn't had made this far.

I'm very obliged to the **Head of Department Prof. Rinku Sharma and all the faculty members of the Applied Physics department** for all the support and guidance. I would like to convey a special thanks to all the PhD Scholars of the LIBT lab.

TABLE OF CONTENTS

LIST OF EQUATIONS

LIST OF FIGURES

ABSTRACT

The development of efficient energy storage devices is crucial in the developing world. A supercapacitor is going to bridge the gap between fast charging electrolytic capacitor and longer charge storage devices like rechargeable batteries. In this report, a polymer-based solid-state supercapacitor is designed and fabricated using silver deposit electrode and PVA/Phosphoric acid-based electrolyte. The electrode material is fabricated using a vapor deposition technique, depositing silver onto the glass substrate at a high vacuum environment. X-ray diffraction (XRD) has been used to identify and confirm the proper phase formation of the crystalline material. Surface characterization has been performed using atomic force microscopy (AFM). In this report, two types of supercapacitor devices are fabricated. In type A supercapacitor, the electrode was made using Ag deposited on a glass substrate, and in type B supercapacitor, the electrode was made using silver deposited on a glass substrate and annealed at 200 °C. A solid-state polymer electrolyte (SPE) is used as an electrolyte-separator medium. Since a solid-state electrolyte is used, therefore the mobility of the dissociated ions in the electrolyte system is reduced affecting the overall specific capacitance of the system. The specific capacitance of Ag deposited on Glass substrate (type A electrode) type supercapacitor is observed 0.71 F/g and for silver deposited on Glass substrate and annealed at 200 °C (type B electrode) type supercapacitor is found 1.05 F/g at a high scan rate of 10 mVs^{-1}.

CHAPTER 1: INTRODUCTION

1.1 Definition

The supercapacitor is an energy storage device that manifests unique properties like high power density, excellent cyclability, fast charge/discharge process, and longer life cycle when compared to the traditional batteries or dielectric capacitor. These types of capacitors consist of a current collector, electrode, separator material, and an electrolyte. Electrochemical Double-Layer Supercapacitor stores charge electrostatically onto the active material. These active materials are designed in such a way that they are electrochemically stable (not reacting to the electrolyte) and have a high specific surface area.

1.2 Background

During the 1950s, engineers of General Electric started experimenting on a porous carbon electrode for better design of fuel cell and rechargeable batteries. In 1957 H. Becker designed an electrolytic capacitor whose electrodes were fabricated using porous carbon material [1]. He explained that the charge in the energy pores is the cause of energy storage. In 1966 engineers of General Electric SOHIO developed an "electrical energy storage apparatus" while experimenting on fuel cell design [2]. SOHIO licensed the technology to NEC who marketed it as "supercapacitors" in 1978 [3]. This product was used as an energy source for memory backup applications.

By the end of the 1980s, enhanced electrode materials extended capacitance values. The evolution of electrolytes with stabler conductivity reduced the equivalent series resistance (ESR) and increased the charge-discharge currents. In 1982 Pinnacle Research Institute (PRI) marketed the first supercapacitor for military applications with low internal resistance.

Recent developments introduce lithium-ion capacitors pioneered by FDK in 2007. Research agencies active in many universities and companies are working to enhance characteristics of supercapacitors such as specific power, specific energy, and cycle stability and to lessen the production costs.

CHAPTER 2: SCIENCE BEHIND SUPERCAPACITOR

The science behind the charge storage mechanism inside a supercapacitor is the separation of charge occurring at the electrode-electrolyte interface (EEI) (4). Helmholtz proposed that the charge double layer is produced at the EEI. This theory was improved by Geary and Stern, and Chapman and Gouy. They proposed that the pilling of ions near the electrode surface is responsible for the presence of the diffusive layer in the electrolyte. The electric double-layer (EDL) structure develops on the surface of the electrode when it is exposed to an electrolytic fluid.
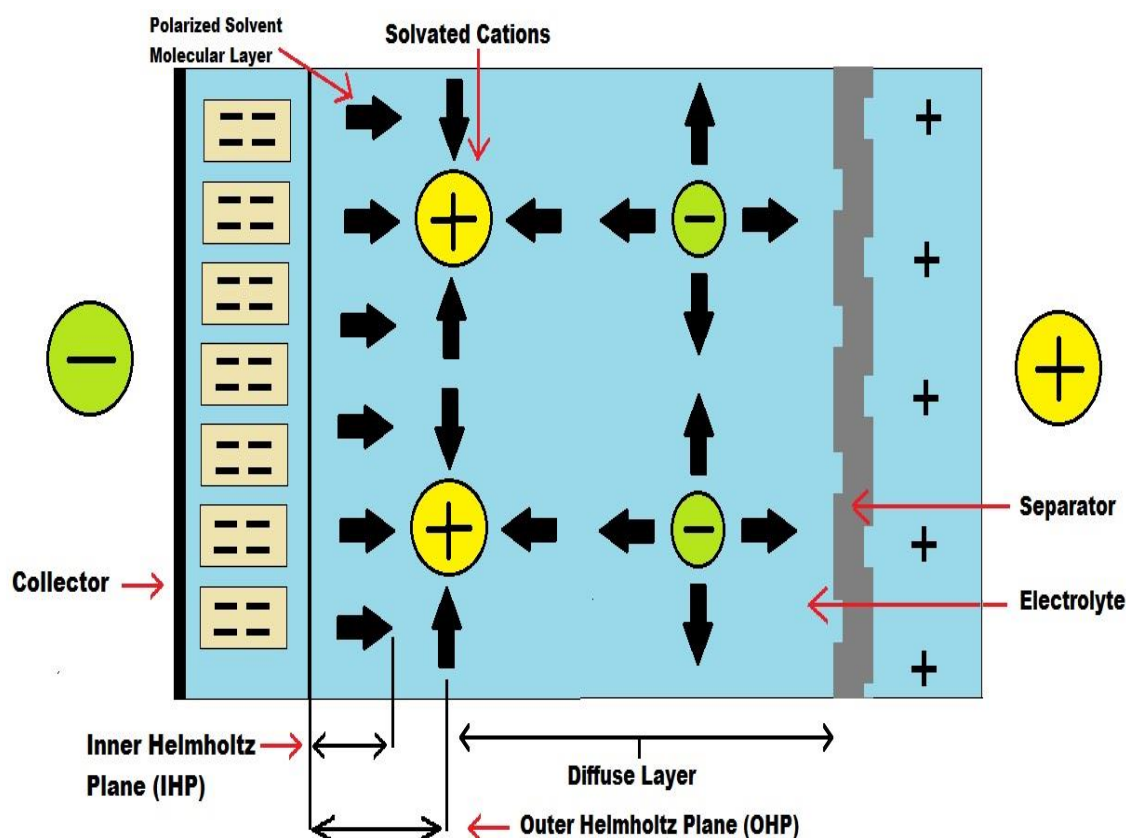

Fig 1: Formation of EDL

An EDL applies to two parallel sheets of charge enveloping the surface of the

electrode. The first layer consists of surface charge (made of ions either positive or negative) captivated onto the surface due to chemical interactions. More the surface area of the electrode more charge will be captivated onto the surface of the electrode (as more sites will be available for chemical interaction). The second layer is called the diffusion layer contains ions drawn to the first layer of surface charge by Coulomb force. The second layer of ions is loosely allied with the electrode surface. A Good electrode material in a supercapacitor device must be highly conductive and should possess a large surface area. The conductivity of the electrode material must be high or else the internal resistance of the supercapacitor will not be in the permissible range [5]. The Supercapacitor has two electrodes that are mechanically divided by a separator and are ionically connected via an electrolyte. The electrolyte is a mix of ions (positive and negative) suspended in a solvent. The solid electrode surface and an adjoining electrolyte interface form a common line (interface). The phenomenon of the double layer effect occurs in this interface.

These types of capacitors consist of a current collector, electrode, separator material, and an electrolyte. Electrochemical Double-Layer Supercapacitor stores charge electrostatically onto the active material. These active materials are designed in such a way that they are electrochemically stable (not reacting to the electrolyte) and have a high specific surface area.

Three factors that influence the double-layer formation are a highly conductive electrode, the high surface area of material, and porosity of electrode (on electrode level). A Good electrode material in a supercapacitor device must be highly conductive and should have a high surface area (for high charge accumulation onto the surface). The conductivity of the electrode material must be high or else the internal resistance of the supercapacitor device will not be in the permissible range [2].

The specific resistance of Ag thin film is quite low making it a good candidate for the Supercapacitor electrode. Ag thin film was grown on a copper substrate

by the vapor deposition method.

CHAPTER 3: ELECTRICAL PARAMETERS

3.1 Capacitance (F)

The Capacitance of the conductors is given by [3]:

$$C = {}^q/_V \quad \ldots\ldots (1)$$

Where:

q = charge held by the conductor,

V = electric potential and is given by:

$$V = \frac{1}{4\pi\varepsilon_0} \int \frac{\sigma}{r} dS \quad \ldots\ldots (2)$$

σ = charge density,

dS = infinitesimal element of area,

r is the length from dS to a fixed-point M within the plate,

ε_O is the vacuum permittivity.

Energy stored inside a capacitor is given by:

$$W_{charghing} = \frac{1}{2} CV^2 \ldots\ldots (3)$$

The capacitance valve is calculated using:

$$C_{total} = I_{discharge} \frac{t_2 - t_1}{v_2 - v_1} \ldots\ldots (4)$$

t2 - t1 is the time difference and v2 − v1 is the potential difference.

3.2 Operating voltage

Operating Voltage Ur is the maximum voltage a supercapacitor can be subjected to so as it operates in the specified temperature range. Higher voltage requires

connecting the capacitor is series to maintain the operating voltage. Above operating voltage comes the breakdown voltage. At breakdown voltage the electrolyte decomposes into its solvent molecules.

So, the operating voltage is greatly determined by the electrolyte used in the supercapacitor.

3.3 Internal Resistance

The movement of charge carriers inside the supercapacitor during the charge-discharge cycle in the electrolyte medium leads to a generation of resistance. This resistance is termed as the internal resistance of supercapacitance and is given by:

$$R_i = \frac{\Delta v_2}{I_{discharge}} \;\ldots\ldots\; (5)$$

 Where:

$\Delta V2$ is voltage drop,

$I_{discharge}$ is discharge current.

3.4 Specific Capacitance

The specific capacitance Cp was calculated using,

$$C_p = \frac{A}{(2mk(v_2 - v_1))} \;\ldots..\; (6)$$

Where:

A is the area under the CV curve,

m is the mass of the active material,

k is the scan rate, and (v2-v1) is the potential window in the CV curve [6-7].

3.5 Current load and cycle stability

In a supercapacitor, reaction constraints do not affect the parameters like current loads, charge, discharge, and peak currents as they operate without forming chemical bonds. This is the reason why the current load and cycle stability of a supercapacitor is higher than a rechargeable batterie. Slower charging and discharging or lower voltage range increases the number of cycles and capacitor life [8].

3.6 Energy capacity

The Energy capacity is the effective amount of energy that can be stored inside a capacitor and is given by W_{eff} (expressed in Joule).

$$W_{eff} = \frac{1}{2}C(V_{max}^2 - V_{min}^2) \ \dots\dots \ (7)$$

Where V represents used voltage.

CHAPTER 4: EXPERIMENTAL SECTION

4.1 Materials and Methods undertaken

The materials utilized during the trials were of scientific standard and used without refinement. The acids used are phosphoric acid (85% wt./vol.), hydrochloric acid (HCl concentration 35.86). PVA and Silver was used as available in lab (high purity materials). Ethanol (CH_3CH_2OH) was purchased and distilled water (DI) was used throughout the process.

4.2 Preparation of solid-state polymer electrolyte (SPE)

1) To make the SPE thin film, 3 gm of phosphoric acid (85% wt./vol.) was taken and was dissolved in 20ml of DI water.

2) The solution was then placed on a hot plate at 85°C and was stirred at the rate of 350 rpm.

3) After a few minutes, 3gm of PVA was added to the solution at the rate of 250 mg per minute to avoid any lump formation.

4) After the complete addition of PVA, the mixture is kept at 85°C at 350 RPM till the PVA is dissolved completely.

5) Once the PVA is completely dissolved the solution was kept inside a hot air oven at 70°C till the mixture becomes clear and does not contain any air bubbles.

6) The mixture was then poured into a glass sheet and bladed to get a film of uniform thickness.

7) Glass sheet containing the mixture was placed in the hot air oven at 30°C

for 12 hr. to dry film completely. Once dried, the SPE film was carefully peeled from the glass sheet.

4.3 Ag coating on Glass substrate

1) The Uniform glass substrate was cleaned with concentrated HCl and DI water to remove any oily residue.

2) After cleaning the glass substrate, it was sonicated for 20 min dipped in DI water. Glass substrate was then dried in a hot air oven. Clean and Spotless glass with the uniform surface was selected for vapor deposition.

3) The glass substrate was coated with Ag by the thermal evaporation technique. Hind Hi-Vac coating unit was used for Ag deposition. Glass substrate was placed on the substrate holder and 50mg of pure silver was placed on the Molybdenum boat.

Fig 2: Thermal Vapor Deposition Unit

1) Both the boat and substrate holder were placed inside the reaction chamber and the chamber was closed to create a vacuum pressure of 10-5 mBar.

2) After obtaining the desired vacuum pressure Ag coating was done onto the Glass substrate until a thickness of 300nm is obtained on the DTM meter (pre-installed functionality of Hind Hi-Vac coating unit).

3) Coating rate was fixed to 5Å/sec ensuring uniform coating onto the glass surface.

4.4 Supercapacitor fabrication

1) In type A supercapacitor, the electrode was made using Ag deposited on a glass substrate.

2) In type B supercapacitor, the electrode was made using silver deposited on a glass substrate and annealed at 200 °C.

3) Peeled SPE film was placed between two Ag electrodes in such a way that two electrodes are not shorted.

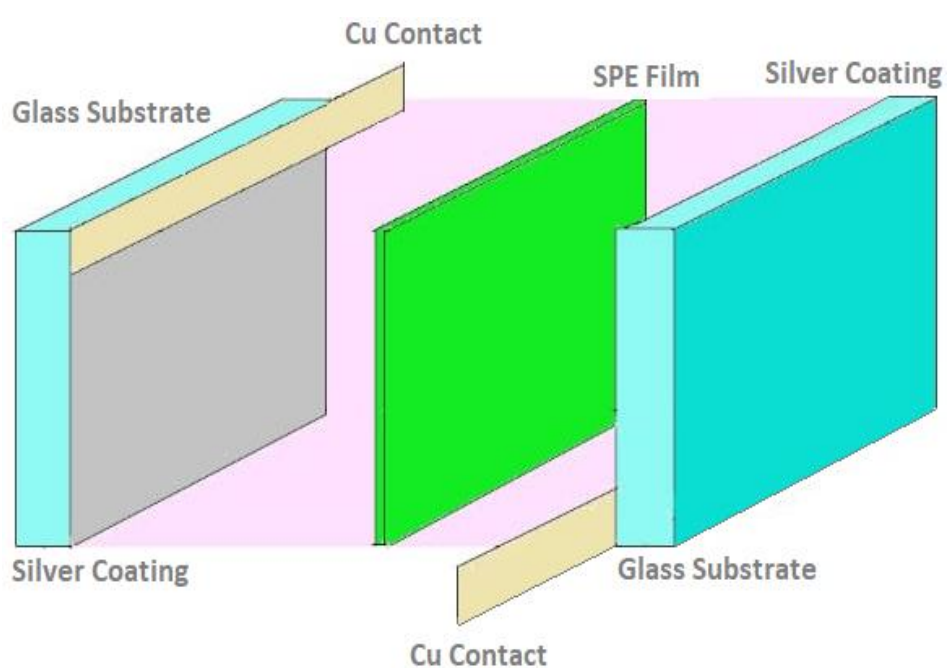4) Cu Contacts are made in the electrode before supercapacitor fabrication.

Fig 3: Supercapacitor Fabrication

CHAPTER 5: CHARACTERIZATION TECHNIQUES

5.1 X-ray Diffraction Method (XRD)

X-ray powder diffractometer (XRD) is a speedy logical technique fundamentally used for level conspicuous verification of a crystalline substance and can give information on single cell approximations. The analyzed matter is accurately grounded, homogenized, and average composed and setup of mass material is resolved.

Basic Concept: Max von Laue, in 1912, found that substances having crystallite popularly travel through as 3-D diffraction grindings for X-shaft ranges like the dislocations of planes in a cross-sectional circle. Currently X-shaft diffraction is regarded as a typical way for the cross examination of precious stone structures and nuclear spacings. Depending on productive interruption of paths of monochromatic beams and the standard substances these beams are created by a CRT, which are kept to deliver monochromatic energies, generally they are collimated so that they can strike, and synchronized with the example. The relationship between the originating beams with the example produces impedance (and a diffracted shaft) fulfilling the Bragg's Law conditions

$$n\lambda = 2d \sin \theta \ \ldots\ldots\ (8)$$

This hypothesis tries to connect the wavelength of em radiation to the diffraction values observed and the cross-sectional divisions of a crystalline standard. After identification these beams are allowed to traverse and then tallied. Upon studying the 2 theta angles and comparing them with the standard ZnO samples we get to know about the various diffraction values that are obtained. This technique helps us in evaluating layer separations present inside the material d. We can even determine the various domains present inside the sample, their homogeneity. The average width regarding their crystallinity can also be calculated from the peak values obtained in the XRD pattern. The in-

plane periodic crystallinity of the plane can also be observed and even the number of layers of the sample present can be evaluated. While observing all these we generally use $CuK\alpha_1$ and $CuK\alpha_2$ as standards for wavelengths which helps in calculating various mathematical formulas and even help in determining FWHM of the sample.
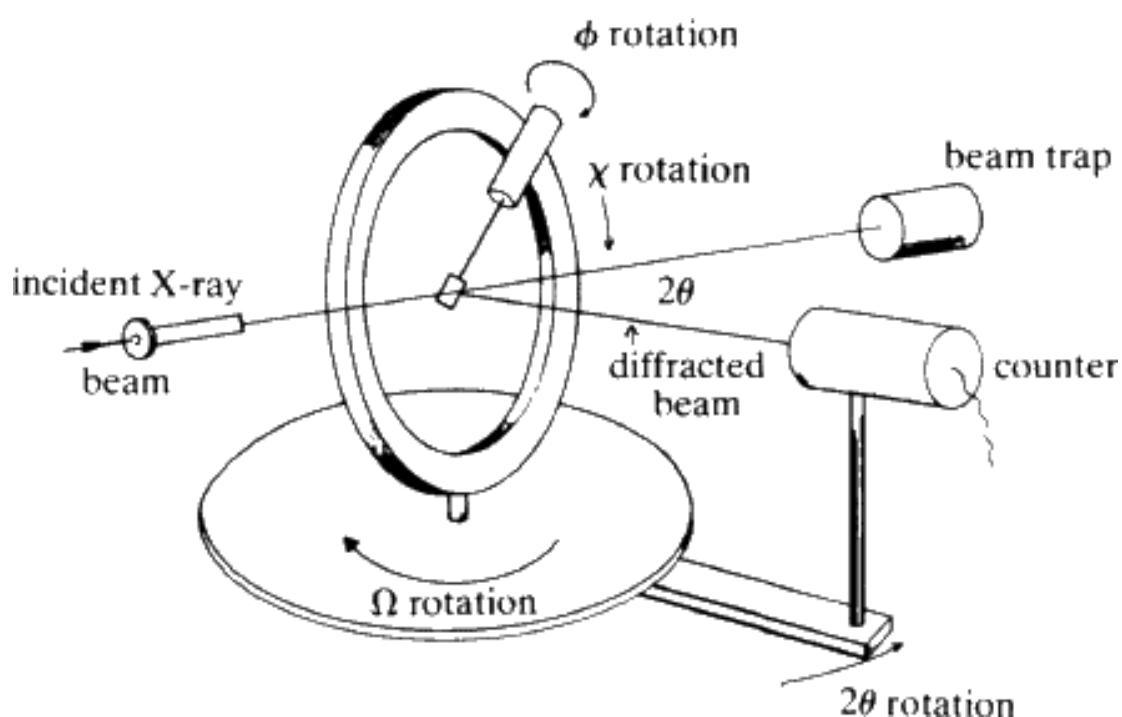

Fig 4: Schematic diagram of XRD working

5.2 Atomic force microscopy (AFM)

Atomic force microscopy (AFM) is an exceptionally high-resolution kind of scanning probe microscopy (SPM),[14] with showed resolution of a nanometer, over many times greater than the optical diffraction boundary. The AFM has

three significant capabilities: topographic imaging, force measurement and manipulation. For imaging, the response of the probe to the powers that the sample forces on it tends to be utilized to frame a picture of the three-dimensional shape of a sample surface. The AFM is used to measure the force between the sample and the probe. The mutual separation is used as a function to measure the force between the sample and the probe. The force spectroscopy and the mechanical properties of the sample are calculated using this function.
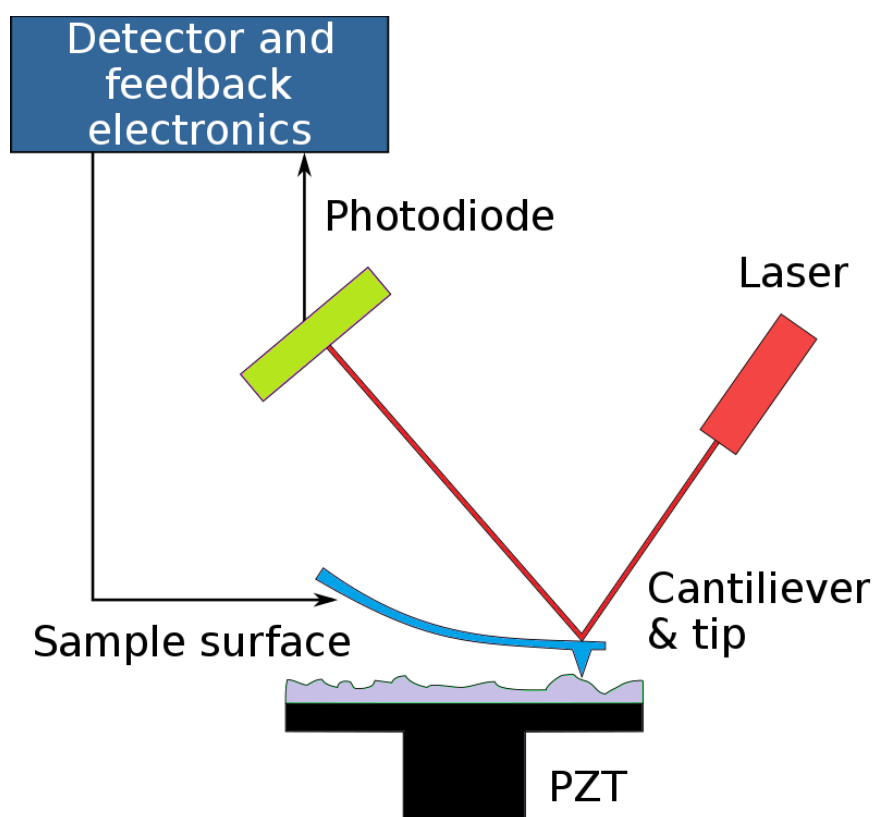
Fig 5: Working of AFM [15]

5.3 Cyclic voltammetry

CV is a kind of potentiodynamic electrochemical measurement. In a CV

experiment, the working electrode potential is ramped linearly versus time. This analysis examines the molecules that are absorbed onto the electrode and are used to study the electrochemical properties of ion's present in the solutions.[16] In CV, the electrode potential inclines straightly versus time in repeating stages. The pace of voltage changes after some time during every one of these stages is known as the experiment's scan rate (V/s). The potential is estimated between the working electrode and the reference electrode, while the current is estimated between the working terminal and the counter terminal. This information is plotted as current (I) versus applied potential (E, frequently alluded to as simply 'potential'). [17-19] During the underlying forward sweep (from t0 to t1) an undeniably decreasing potential is applied; accordingly, the cathodic current will, at any rate at first, increment over this timespan expecting that there are reducible analytes in the framework. Eventually, after the decreased capability of the analyte is reached, the cathodic current will diminish as the convergence of the reducible analyte is exhausted. On the off chance that the redox couple is reversible, at that point during the converse output (from t1 to t2) the diminished analyte will begin to be re-oxidized, offering to ascend to a current of an opposite extremity (anodic current) to previously. The more reversible the redox couple is, the more comparative the oxidation pinnacle will be fit as a fiddle to the decrease top. Subsequently, CV information can give data about redox possibilities and electrochemical response rates.

5.4 Electrochemical Impedance Spectroscopy

Electrochemical impedance spectroscopy (EIS) is a valuable method to investigate electrochemical systems such as batteries. For a battery, where potential perturbations of varying frequency are applied on an electrode, the impedance response can give critical insights in battery processes as:

- Capacitance, electrochemical reactions, and local resistances which are short time-scale processes affect the impedance at high frequencies. [10]

- Whereas, at low frequencies, diffusion in the electrolyte and active material particles (i.e., large time-scale processes) contribute to the impedance.[11]

Nyquist plots are representation of frequency dependent entities such as impedance, voltage gains, system transfer functions in complex plane in polar coordinates.

Chapter 6: RESULTS & DISCUSSIONS

6.1 X-ray Diffraction (XRD)

X-ray diffraction (XRD) patterns of the Ag thin film coated on Glass substrate is obtained at room temperature and is shown in Figure. The observed XRD patterns are compared with the standard XRD pattern (JCPDS card. No. 89-3722) of Ag. By comparing to the standard XRD pattern of the Ag, the peaks at 38.2°, 44.3°, 64.7°, and 77.5° can be attributed to the Miller indices of (111), (200), (220), and (311). It has been noticed that the proper phase (face-centered cubic structure) of Ag is formed.
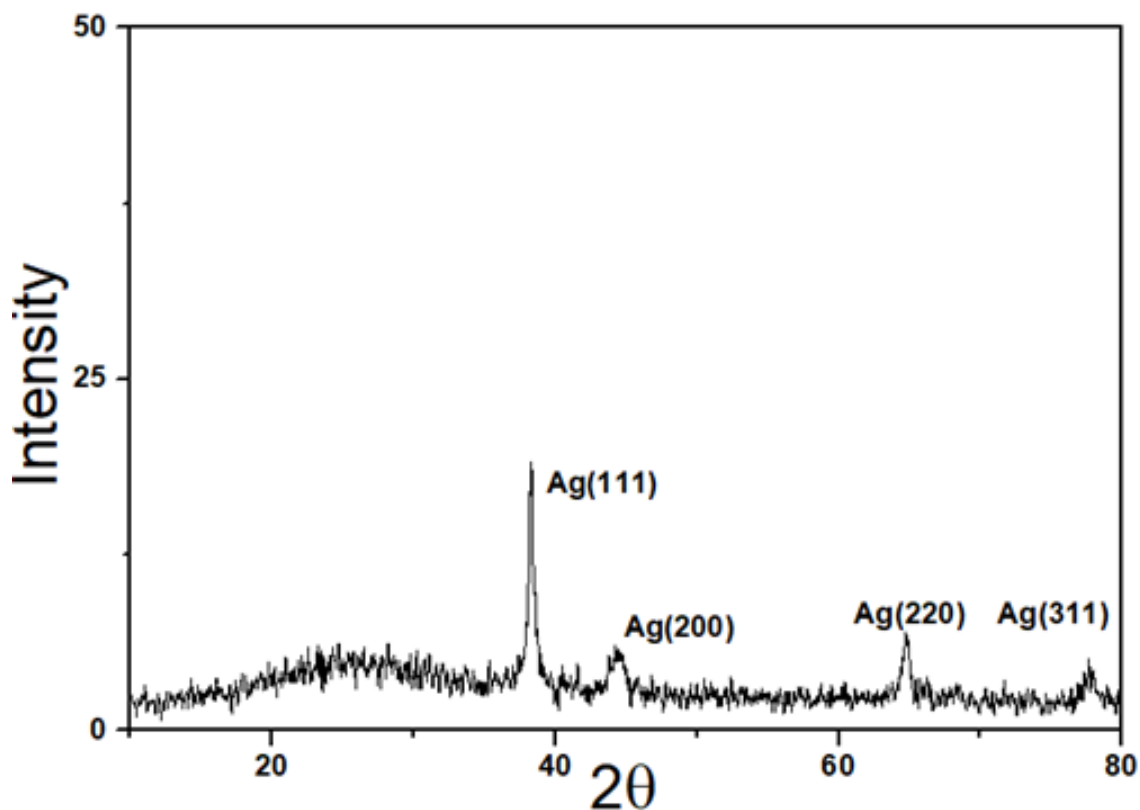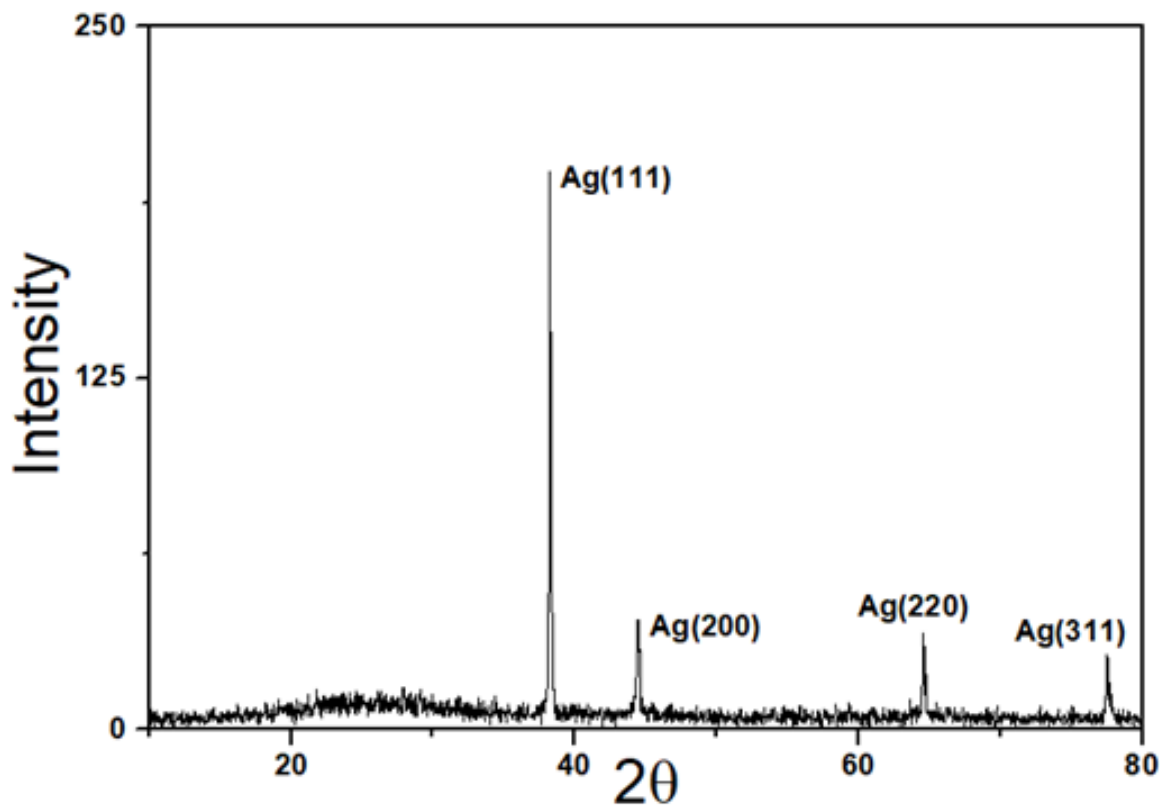

Fig 6: XRD of type A silver electrode

Fig 7: XRD of type B silver electrode

It is visible from the XRD pattern that when the substrate was annealed at 200° C, peak intensity increased. The average crystalline size was calculated from XRD data using the Scherrer Equation. For type A electrode, the crystalline size was 15.66 nm and 50.7 nm for the type B electrode.

3.2 Atomic force microscopy (AFM)

The surface morphology was studied by atomic force microscopy. The surface texture of the Ag deposited on Glass substrate in 3D is shown in Figure.
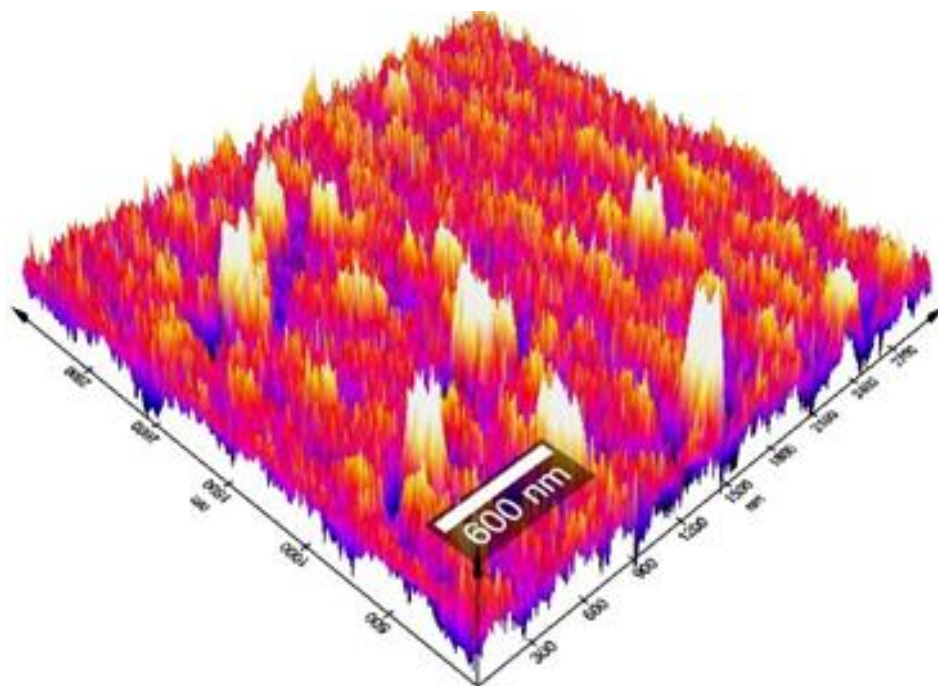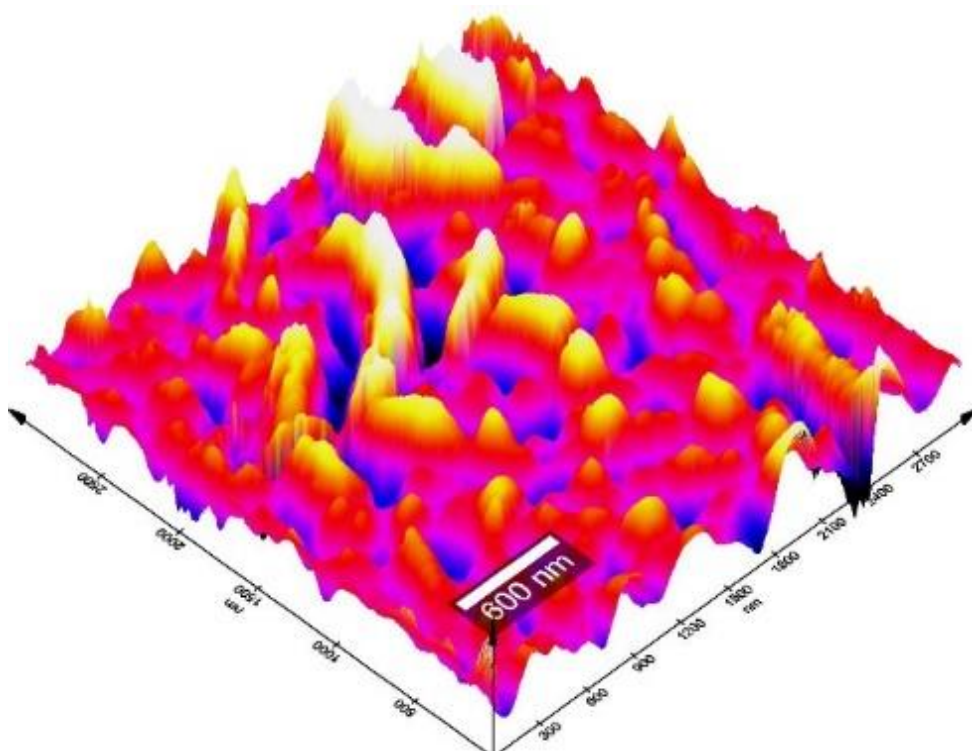
Fig 8: AFM of type A silver electrode

Fig 9: AFM of type B silver electrode

Skewness of the 3D surface texture was computed, which indicates the degree of symmetry of the surface heights about the mean plane or base. The sign of SSK symbolizes the supremacy of peaks (SSK>0) or valley structures (SSK<0) covering the surface. SSK value for the type A electrode is 0.59264 and of type B electrode is 0.07588.

3D image of the scanned surface by AFM technique shows that type A electrode material is highly rough as compared to type b. Annealing at 200 °C caused the rough surface to smooth out.

3.2 Electrochemical performance

Charge–discharge response of the supercapacitors was evaluated by CV measurement. CV measurement was obtained for the fabricated SPE Capacitor. CV curve was obtained for different scan rates within the potential range of 0-0.5 V. The distinctive rectangular shape of the CV curve implies that the charge was accumulated at the electrode-SPE interface forming an electric double layer.
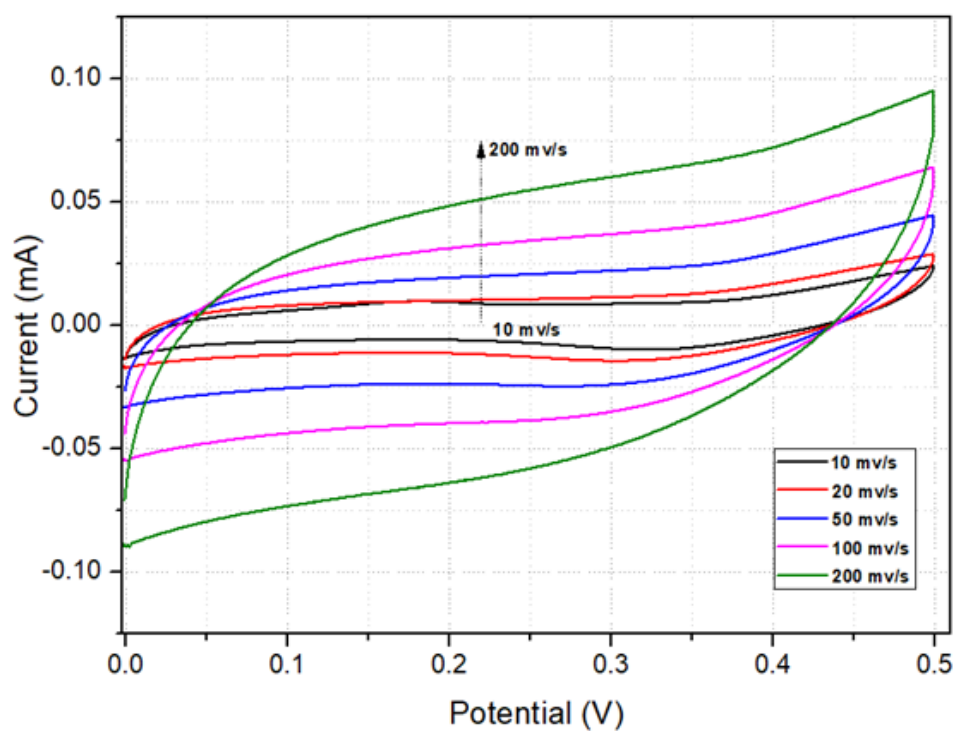
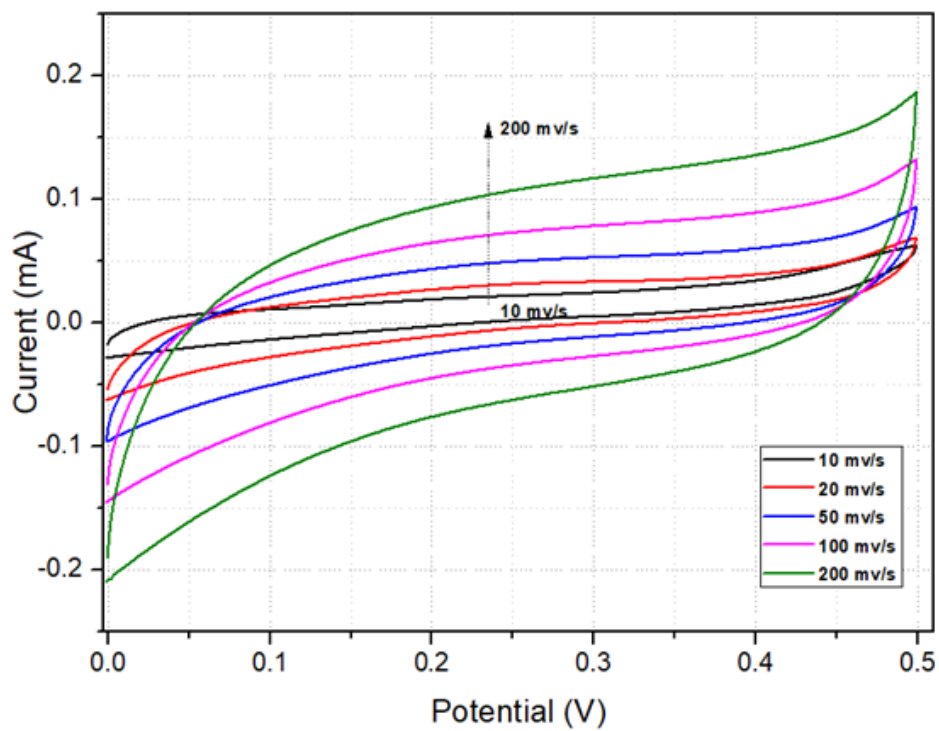**Fig 10:** Cyclic Voltammetry of type A supercapacitor

Fig 11: Cyclic Voltammetry of type B supercapacitor

The distinctive rectangular shape of the CV curve implies that the charge was accumulated at the electrode-SPE interface forming an EDL. The CV curve retained its rectangular shape with an increase in scan rate from 10 mVs-1 to 200 mVs−1. The mass of the silver deposited on the electrode was used to compute the Cp of the fabricated supercapacitor. The quantity of silver deposited on an electrode was quite low at approximately 1 mg for 9.375 cm2. Specific Capacitance (Cp) was calculated using,

$$Cp = \frac{A}{(2mk(v2-v1))} \ \ldots\ldots\ (9)$$

Where A signifies the area under the CV curve, k implies the scan rate, m means the mass of the active material, and (v2-v1) value holds the potential window of the CV curve.

The Cp of type A supercapacitor is around 0.71 F/g and of type B supercapacitor is around 1.05 F/g at a high scan rate of 10mv/sec. The value of Cp increased as the scan rate decreased. This phenomenon can be associated with the reduced efficiency of ion diffusion at the EEI as the scan rate is increased.

Due to its accuracy and non-damaging effects, Electrochemical impedance spectroscopy (EIS) is a very feasible and also the most preferred method for obtaining the impedance characterization of Li-ion batteries, For EIS, a sinusoidal varying potential at different frequencies, but fixed peak-to-peak voltage is applied across the battery terminals, the output response is a function of frequency and can be studied using any frequency domain analysis tools . For low frequencies, the resistances dominate over other transient elements such as capacitances, thus, impedance spectroscopy looks like a straight line with a constant slope.
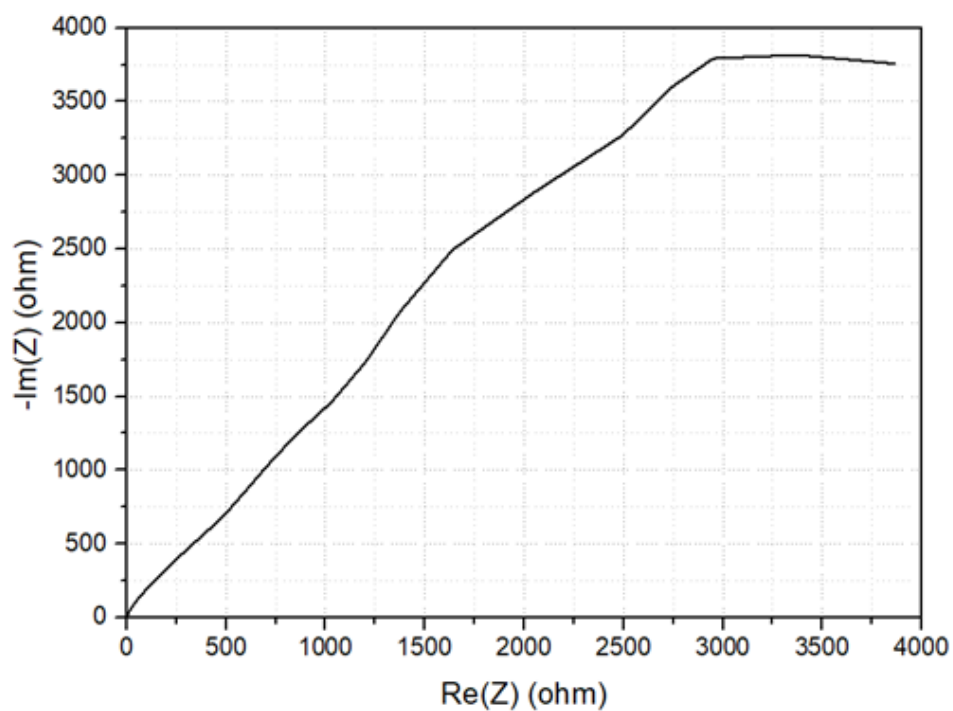
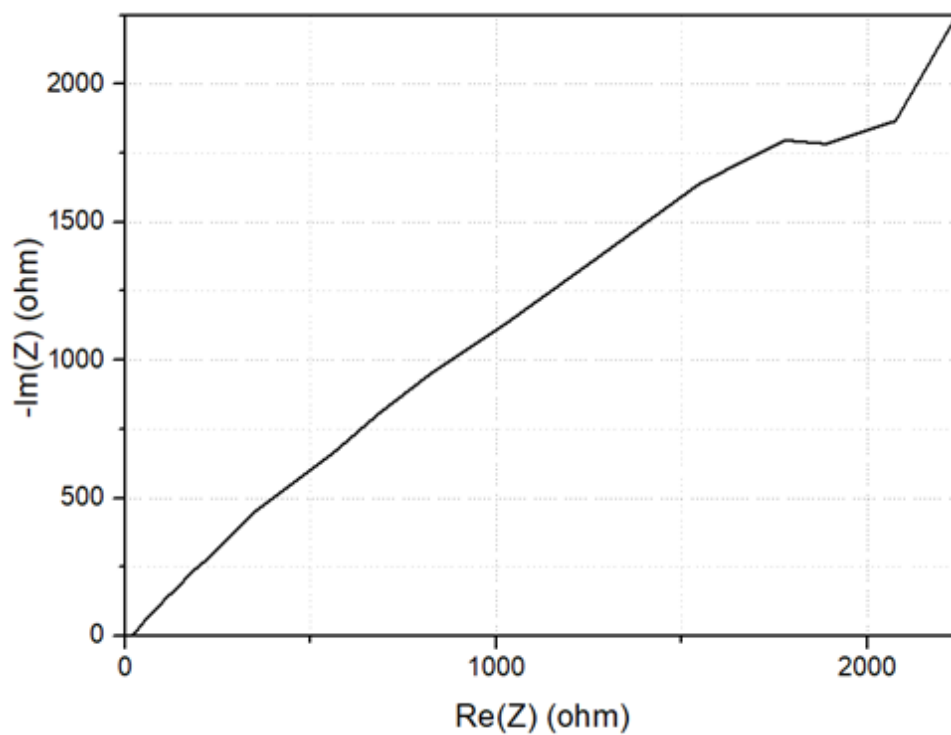**Fig 12:** Nyquist plots of type A supercapacitor

Fig 13: Nyquist plots of type A supercapacitor

EIS measurements were taken for both types of the supercapacitor. The impedance data were taken at the open circuit potential by employing the alternating potential of an amplitude of 5mV atop a scale of frequencies from 100 kHz to 150 mHz. CV performance of both type A and type B supercapacitor is quite different in terms of specific capacitance. Cp of type B supercapacitor is higher than type A supercapacitor.

The EIS curve shows that the impedance of the type B capacitor is lower than type A. This can be explained by the surface continuity of type B supercapacitor due to annealing. Annealing of the silver electrode has reduced the roughness of the surface which can be attributed to lower surface to volume ratio but the surface becomes more continuous and conductive. This led to increase in Cp in type B supercapacitor.

CONCLUSION

Supercapacitors are a crucial component of several applications like communication devices, electric vehicles, UPS, mobile phones, etc. Supercapacitors will thrive because of their numerous technological gains like quick charging and discharging processes, exceptional cycle stability, and high-power densities, etc.

In the developing world, technologies demand larger measures of energy to be collected within a shorter period but at a lower cost. A supercapacitor can play a critical role in spanning the gap between fast charging and longer charger storage.

As the energy demand of the world is increasing, it is now crucial to develop efficient energy storage devices. Though nanotechnology has opened new areas in the field to material science, different materials need to be exploited to increase the efficiency and overall performance of supercapacitors. Although many supercapacitors are developed exploiting various nanomaterials structures, research on silver-based thin-film supercapacitors is at the nascent stage. In this paper, we have designed a supercapacitor based on silver and polymer film.

REFERENCES

[1] Ho, J.; Jow, R.; Boggs, S. (Jan 2010). "Historical Introduction to Capacitor Technology" (PDF). IEEE Electrical Insulation Magazine. 26 (1): 20–25. doi:10.1109/mei.2010.5383924.

[2] A brief history of supercapacitors AUTUMN 2007 Batteries & Energy Storage Technology Archived 2014-01-06 at the Wayback Machine

[3] US 3288641, Rightmire, Robert A., "Electrical energy storage apparatus", issued 1966-11-29

[4] Li Li Zhang and X. S. Zhao, Chem. Soc. Rev., 2009,38, 2520-2531

[5] Simon, P., Gogotsi, Y. Materials for electrochemical capacitors. Nature Mater 7, 845–854 (2008).

[6] E. Taer "Eggs Shell Membrane as Natural Separator for Supercapacitor Applications", Advanced Materials Research Vol. 896 (2014) pp 66-69"

[7] Y. M. Shulga, S. A. Baskakov, V.A. Smirnov, N.Y. Shulga, K.G. Belay and G.L. Gutsev: J. Power Sources, 245(2014), 33-36.

[8] Waseem Raza, Nano Energy 52 (2018) 441–473

[9] Zhang, Sanliang & Pan, Ning. (2014). Supercapacitors Performance Evaluation. Advanced Energy Materials. 5. 10.1002/aenm.201401401

[10] Chen, Tao & Dai, Liming. (2013). Carbon nanomaterials for high-performance supercapacitors. Materials Today. 16. 272-280. 10.1016/j.mattod.2013.07.002.

[11] Maxwell BOOSTCAP Product Guide – Maxwell Technologies BOOSTCAP Ultracapacitors– Doc. No. 1014627.1 Maxwell Technologies, Inc. 2009

[12]   Liang, M., & Zhi, L. (2009). Graphene-based electrode materials for rechargeable lithium batteries. Journal ofMaterials Chemistry, /9(33), 5871-5878.

[13]   Moretti, A., Kim, G. T., Bresser, Renger, K., Paillard, E., Marassi, R., & Passerini, S. (2013). Investigation of different binding agents for nanocrystalline anatase TiO2 anodes and its application in a novel, green lithium-ion battery. Journal ofPower Sources, 221, 419-426.

[14]   https://en.wikipedia.org/wiki/Atomic_force_microscopy

[15]   https://en.wikipedia.org/wiki/X-ray_crystallography

[16]   Bard, Allen J.; Larry R. Faulkner (2000-12-18). Electrochemical Methods: Fundamentals and Applications (2 ed.). Wiley. ISBN 978-0-471-04372-0.

[17]   Nicholson, R. S.; Irving. Shain (1964-04-01). "Theory of Stationary Electrode Polarography. Single Scan and Cyclic Methods Applied to Reversible, Irreversible, and Kinetic Systems". Analytical Chemistry. 36(4): 706–723. doi:10.1021/ac60210a007.

[18]   Heinze, Jurgen (1984). "Cyclic Voltammetry-"Electrochemical Spectroscopy". New Analytical Methods (25)". Angewandte Chemie International Edition in English. 23 (11): 831–847. doi:10.1002/anie.198408313.

[19]   Elgrishi, Noémie; Rountree, Kelley J.; McCarthy, Brian D.; Rountree, Eric S.; Eisenhart, Thomas T.; Dempsey, Jillian L. (3 November 2017). "A Practical Beginner's Guide to Cyclic Voltammetry". Journal of Chemical Education. 95 (2): 197. Bibcode:2018JChEd..95..197E. doi:10.1021/acs.jchemed.7b00361.